KERNFORSCHUNGSANLAGE JÜLICH GmbH
Institut für Plasmaphysik
Association EURATOM-KFA

Characteristics of a High Current Ion Source Operated with Lithium

by

H. L. Bay, E. Dullni and P. Leismann

Jül - 2062
May 1986
ISSN 0366-0885

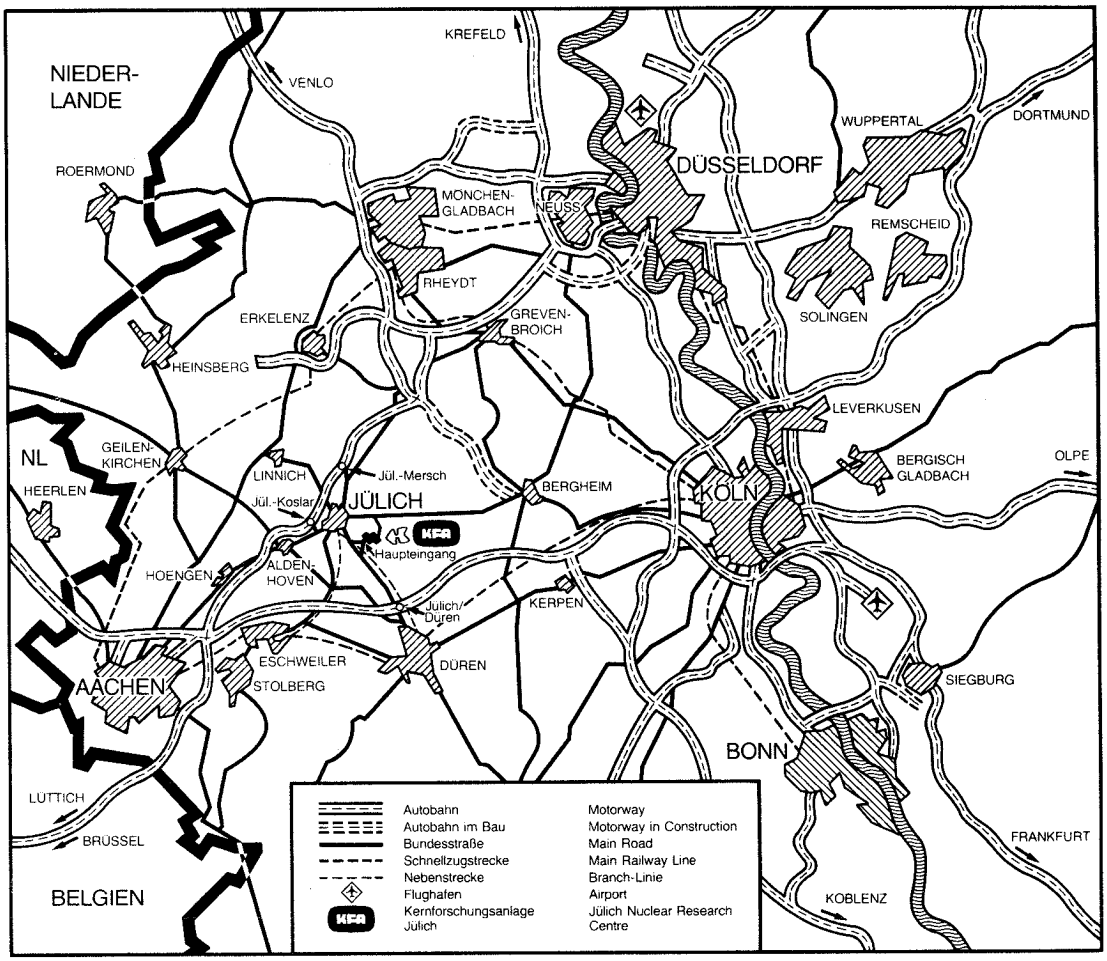

Als Manuskript gedruckt

Berichte der Kernforschungsanlage Jülich – Nr. 2062

Institut für Plasmaphysik Association EURATOM-KFA Jül - 2062

Zu beziehen durch: ZENTRALBIBLIOTHEK der Kernforschungsanlage Jülich GmbH

Postfach 1913 · D-5170 Jülich (Bundesrepublik Deutschland)

Telefon: 02461/610 · Telex: 833556-0 kf d

Characteristics of a High Current Ion Source Operated with Lithium

by

H. L. Bay, E. Dullni and P. Leismann

Characteristics of a High Current Ion Source Operated with Lithium

H.L. Bay
Institut für Plasmaphysik, KFA Jülich, Ass. EURATOM-KFA, 5170 Jülich

E. Dullni[1], P. Leismann
Institut für Experimentalphysik V, Ruhr-Universität Bochum,
4630 Bochum

Abstract

A low pressure arc ion source has been tested for operation with lithium. Currents up to 120 mA could be extracted through a multiple aperture extraction system at energies of 30 keV. The ion beam was neutralized up to 70 % in a charge exchange cell filled with lithium vapour. The beam divergence ranged from 20 to 25 mrad full angle deduced from the spatial distribution of the collision induced Li I resonance line. Current densities from 2 to 3 mA/cm^2 at a distance of 1.9 m from the source were measured either by laser induced fluorescence or with a Faraday cup.

[1]Present address:
Brown Bovery & Cie, Research Center, CH-5405 Baden-Dättwil, Switzerland

Contents

1. Introduction

Recently, neutral beams have been proposed for diagnostic measurements in fusion plasma devices. From charge exchange, ionization and excitation reactions with ions of several kinds the respective ion densities can be deduced [1,2]. The attenuation of the injected beam allows for the determination of the electron or proton density in the vicinity of the plasma edge [3]. Lithium has been chosen for such a beam, since it has the highest charge exchange cross-sections [4]. It can be tolerated as a plasma impurity within certain limits, because it only gives a minor contribution to the effective Z.

For the feasibility of the charge exchange measurements, an equivalent neutral current density of up to 5 mA/cm^2 and an energy around 30 keV are needed. Since only ionized particles are extracted from an ion source, but neutrals are needed, the ion beam has to be neutralized by charge exchange in Li- or Na-vapour [5].

McCormick et al. [6] have developed and tested a lithium ion source based on the Li-ion emission of a heated solid surface (beta-Eucryptite). For a beam energy of 27 keV, they obtained a neutral beam current of 0.16 mA at a distance of 1.65 m from the source. The diameter of the beam was 8 to 9 mm. The current was limited by the Pierce-extraction geometry used. Weber [7] succeeded in modifying a duopigatron ion source to supply a lithium ion current of several milliamperes.

Keller et al. [8] have developed a hot cathode ion source named HORDIS (Hot cathode Reflex Discharge Ion Source) for operation with non-volatile elements (mainly alkaline metals Bi, Ca). It can be operated with all elements having a vapour pressure exceeding 1 mbar at 1200 °C. Its operation is briefly described as follows: A low-pressure arc sustained by heated filaments is burning in argon. When the walls of the discharge chamber are heated up by the filaments and the arc itself, the non-volatile material, as e.g. lithium, is evaporated in a separate furnace and diffuses into the discharge chamber.

In this report, the operational characteristics of this source are described in detail. The stress is layed on the special problems originating from the operation with a non-volatile material, i.e. Li. The Li-beam was mainly analysed after being neutralized in the charge exchange cell in view of the later application as a diagnostic beam at TEXTOR as mentioned above. Its spatial profile was determined from the spatial distribution of the fluorescence light emitted by Li I at 671 nm. This line is excited in collisions with background gas atoms. From these profiles, the neutral beam divergence has been calculated. The ion beam current was measured by a Faraday cup. Because of the high space charge density existing in the beam these measurements need special care. Thus, Faraday cup measurements have been combined with calorimetric, spectroscopic and laser excitation measurements.

2. The Low-Pressure Arc Ion Source

2.1 Construction

The ion source, which has been developed in the GSI Darmstadt has been described in ref. 8 and only some of the main features will be mentioned in the following discussion (Fig. 1). The operation of the source is usually started with a pure argon discharge. The gas feed is positioned in the rear part of the source. During operation we control the Ar gas supply by the pressure measured directly at the gas feed, which is a factor of 37 higher than that existing in the discharge chamber. This was checked by properly positioned Pirani vacuum tubes. For a reading of 0.06 to 0.1 mbar, the pressure in the discharge chamber is between 1.3 and 2.2 μbar. (It has to be remembered that for Ar the pressure reading of the thermovac has to be multiplied by a factor of 1.5 in order to get the real pressure.) In the following, we always refer to the real pressure measured at the gas feed. A low pressure arc in a cylindrical discharge chamber is sustained by the hot cathode consisting of six tantal filaments, and it is ignited when the potential on the cylindrical anode exceeds 25 V. A multipole magnetic field of about 10 mT increasing towards the walls impedes the diffusion of electrons. The discharge voltage can be modulated by a rectangular puls generator in

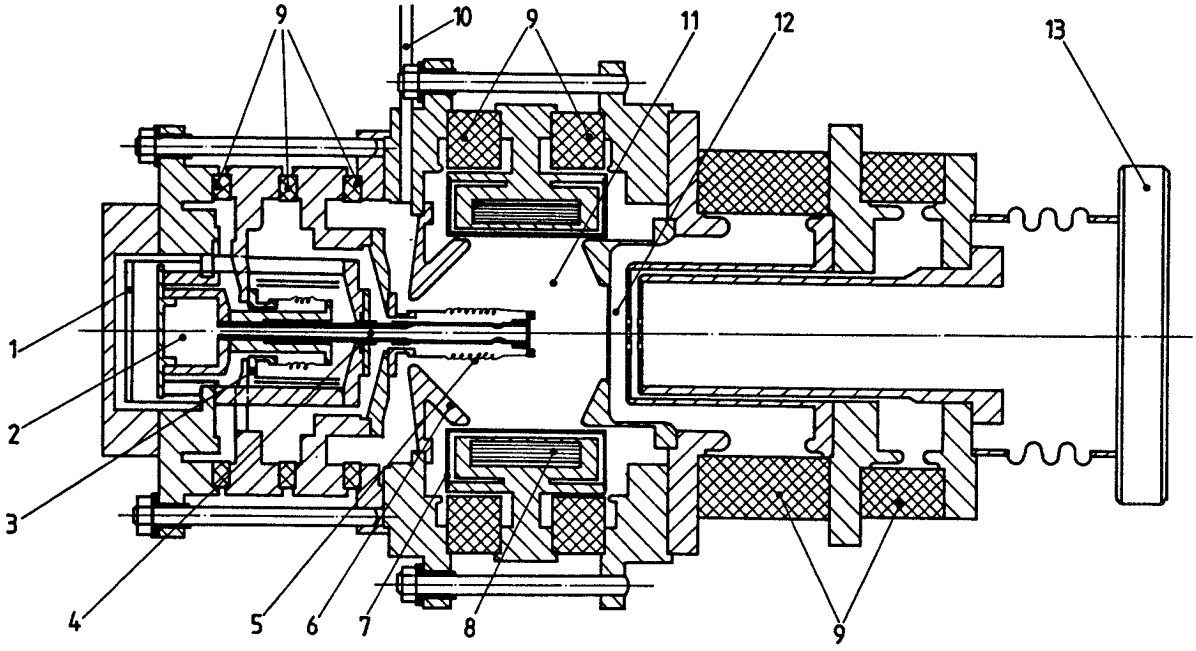

Fig. 1: The HORDIS ion source. 1 Heat shields. 2 Oven with removable cap. 3 Oven heating. 4 Hot cathode pipe (Mo) for the vapour inlet into the discharge chamber. 5 Filaments. 6 Rear reflector. 7 Anode cylinder (Mo). 8 Permanent magnets. 9 Isolators. 10 Gas inlet tube. 11 Discharge chamber. 12 Extraction grids. 13 Mounting flange.

order to get a pulsed ion beam. The minimum pulse duration is 100 µs determined by the rise and fall time of the arc current supply. In the present version the ions are extracted through seven holes, 5 mm in diameter and arranged in a hexagonal hole pattern with the centerhole on axis.

The pressure outside the ion source is only 15 % of that inside because of the limited pumping conductance of the extraction holes. A low pressure outside is desirable in order to prevent spreading of the ion beam by collisions. The extraction grid and the rear reflector have direct contact to the plasma and assume the potential of the cathode (Fig. 2). The whole ion source including the extraction grid is kept on positive potential. Plasma ions at the holes are accelerated by the electric

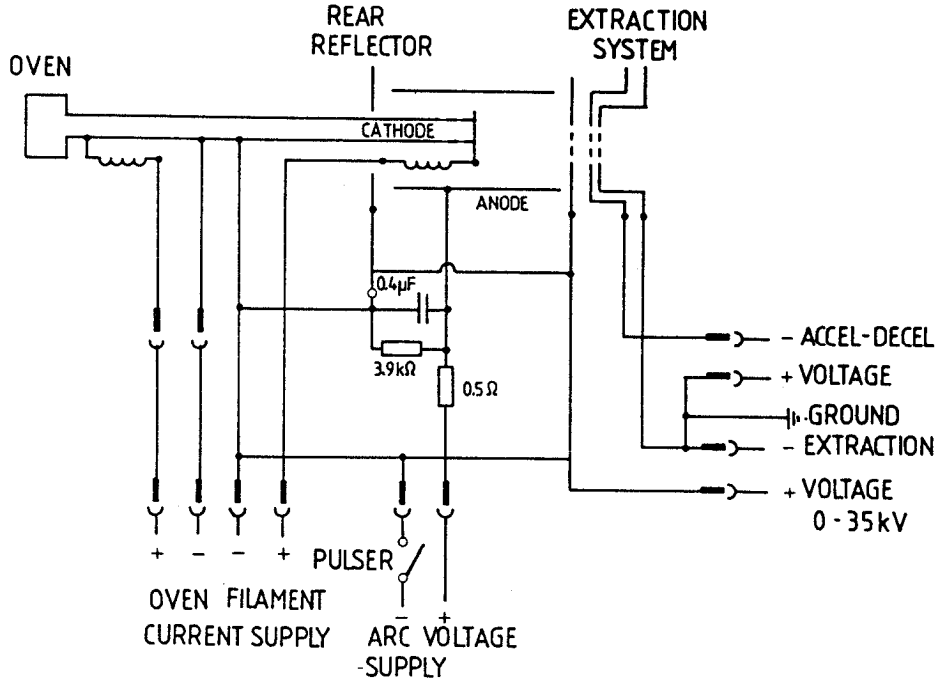

Fig. 2: Wiring diagram of the ion source.

field and a concave curved plasma surface (Langmuir-sheath) will be formed. The extraction system was designed for a maximum extraction voltage of 50 kV [8], but in the present investigation it was limited to 35 kV by the high voltage power supply. The second grid was kept on a potential of -1 kV and the third grid on ground. This acceleration-deceleration system prevents electrons in the beam from being accelerated into the source producing X-ray radiation. The holes in all three grids are drilled through in one turn to facilitate their alignment. The two charged grids are separated by a gap of 7.5 mm and the second and third grids by 1 mm.

The walls of the discharge chamber have a poor thermal contact to the water-cooled flanges. (The flanges have O-ring sealings.) This is especially true for the thin anode cylinder made of Mo (Fig. 1). It must be heated up to temperatures of more than 400 °C in order to prevent condensation of lithium. Solid lithium is evaporated in a separate furnace which is connected to the discharge chamber by a tube of 5 mm inner diameter. The furnace is heated by a set of tungsten wires grouped around the connection tube. The coolest wall determines the vapour

pressure of lithium achievable in the discharge chamber. By thermocouples temperatures up to 750 °C at the rear reflector (Fig. 1) and up to 550 °C at the front reflector which holds the extraction grid were measured. This allows for a lithium vapour pressure of at least 1.3 μbar (see appendix) and probably more, since we expect a thermal gradient between the surface facing the plasma and the location of the thermocouple.

2.2 Operational Characteristics

The ion source has three main operation modes which depend on the feeding gas.

A. Pure argon operation
B. Operation in a mixture of argon and lithium
C. Pure lithium operation.

These three modes are not strictly separated, but they more or less merge depending on the arc discharge parameters. These parameters are optimized for an extraction voltage of 30 kV, for a maximum current density and for an almost rectangular pulse-shape.

The maximum current extracted from a single hole of diameter d is given by the Child-Langmuir relation for space-charge limited current [9].

$$J = \pi \varepsilon_0 \cdot d^2/9 \cdot (2e/M)^{1/2} \cdot (U^{3/2}/l^2) \qquad (1)$$

M is the mass of the extracted ions (in kg) and U the applied voltage. l is the spacing of two adjacent flat plates or the extraction grids, as in our case. Since the holes distort the electric field, l must be corrected by the following expression [10]:

$$l^2 = l_e^2 + d^2/4$$

with l_e being the geometric spacing of the grids. For the grids used here and argon, we calculate a total current of $\sim$ 100 mA.

The duty-cycle of the pulsed arc may not be chosen too low, since otherwise the electric power is insufficient to heat up the walls of the discharge chamber. Thus duty-cycles of 20 - 50 % depending on the operation mode were used. Shorter as well as longer pulses up to continuous operation are in principle possible, though the heat load may be too high in the latter case. The periods ranged between 10 and 40 ms. Operation at higher repetition rates has been tested, but if rectangular pulses are wanted, the pulse length should be chosen to be $\gtrsim$1 ms due to the finite risetime.

2.2.1 Pure Argon Operation

In the pure argon mode the argon pressure at the gas feed is between 0.1 and 0.15 mbar (Table 1). The extracted current is about 55 mA, which is a factor of 2 smaller than that calculated from the Child-Langmuir relation. The current is obtained from the meter reading of the high voltage supply unit diminished by the leak current through the water tubes, which supply the cooling of the ion source, and that produced by ions hitting the intermediate grid. The result is then devided by the duty-cycle.

Table 1
Typical parameters for the three operation modes of the ion source

mode	A	B	C	unit
rel. Ar pressure	100	50-70	0-30	%
furnace temperature	$\angle$ 300	600-680	680-750	°C
filament current	150-160	150-160	140-150	A
discharge current	20	20	30	A
discharge voltage	50-60	40-60	20-40	V
extr. ion current	$\angle$ 55	55-80	80-120	mA
intermed. grid current	5	1.5	$\angle$ 1	mA
Li fraction	0	5-50	50-100	%

The cathode heating current typically is about 150 to 160 A for new tantal filaments, the arc voltage is between 50 - 60 V and the arc current about 20 A. The extracted beam has a smooth pulse-shape with a rise-time of $\lesssim$ 2 ms. The pulse-shape sensitively depends on the argon pressure, the discharge voltage and the filament heating current. A shorter rise-time always causes a lower plateau value of the current. This must be due to the different conditions for igniting the plasma and maintaining it.

2.2.2 Operation in a Mixture of Argon and Lithium

When the furnace is heated up for about 30 to 45 min and Li vapour starts to diffuse into the chamber, the Ar gas pressure can be reduced

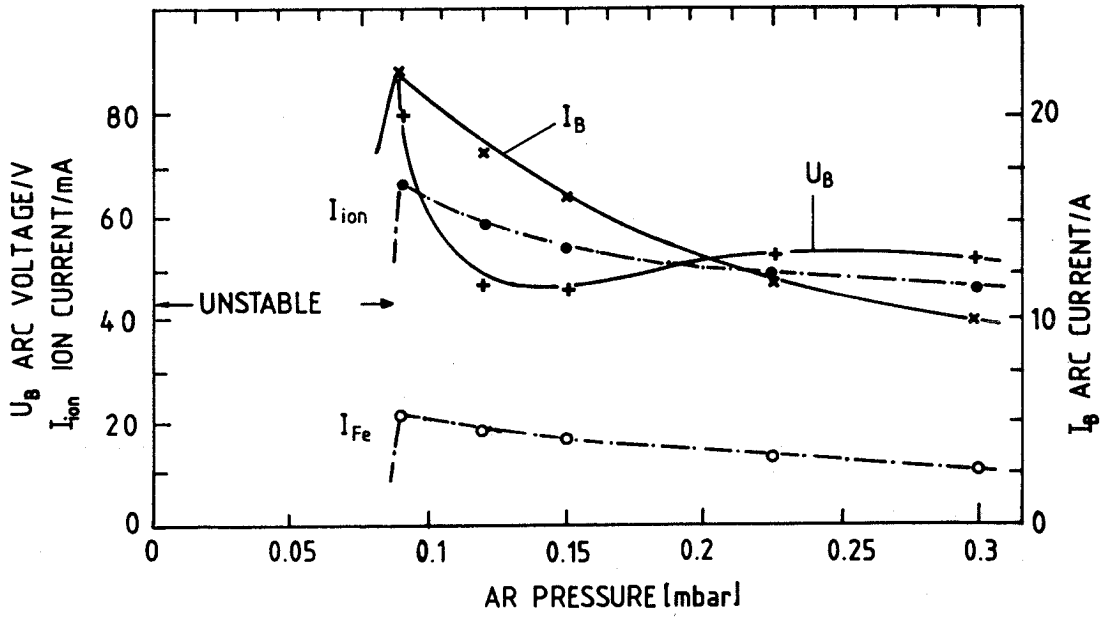

Fig. 3: Discharge parameters of the operation mode B as function of the pressure. The Ar pressure in the discharge is about a factor 38 lower (see text). The ion current I_{ion} is the extracted beam current, I_{FC} the current at the Faraday cup. The data were taken with an oven temperature of 680 °C and a filament heating current of 150 - 160 A.

by 30 to 40 %. The risetime of the extracted beam pulse decreases, and very often ~100 kHz oscillations appear on both the arc voltage and the beam current. In this mode, the temperature of the furnace is not high enough to supply as much lithium as is needed for a pure Li plasma and the beam consists of some fraction of Li and Ar. This is evident when the Ar pressure is further reduced: the discharge distinguishes (Fig. 3). From different considerations explained in section 4.2 we conclude that argon still constitutes a fraction of 50 to 90 % of the beam. The argon concentration of the Li-beam would not complicate the measurements at TEXTOR, but for other reasons an analyzing magnet will be installed between the extraction and the neutralization cell supplying a mass separated pure Li-beam. For the present investigations, however, this magnet was not available.

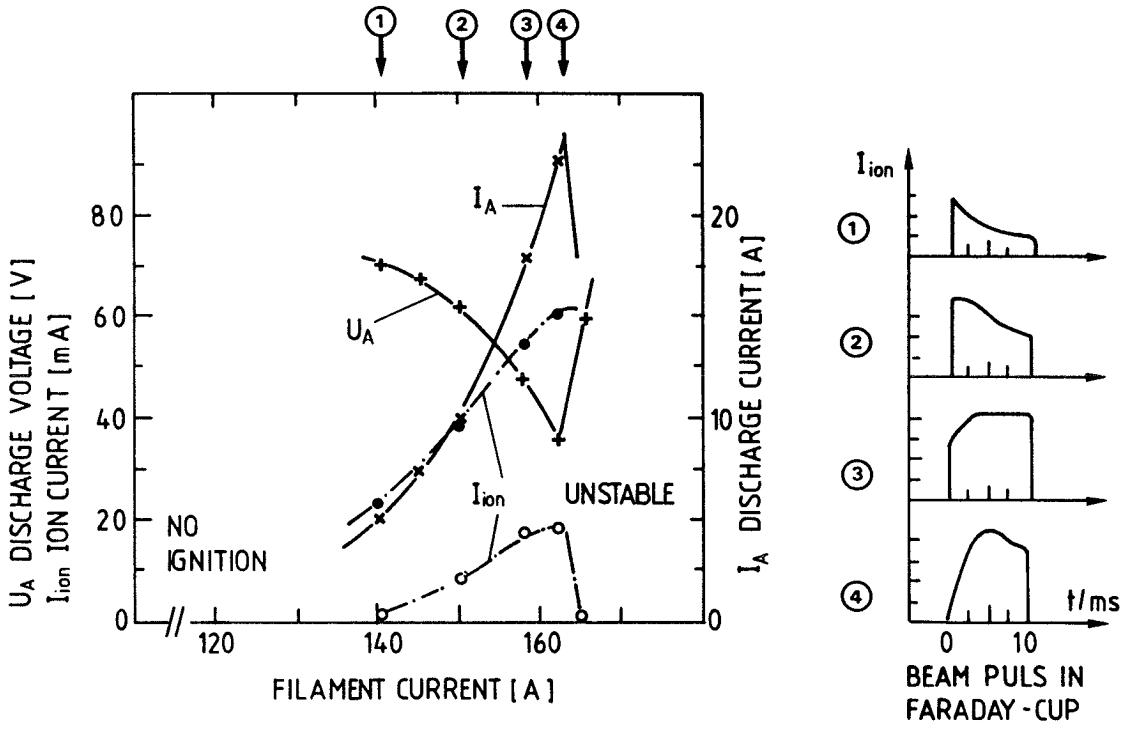

Fig. 4: Discharge parameters of the operation mode B as a function of the filament heating current. On the right typical pulse-shapes of the Faraday cup current are shown. The data were obtained for an oven temperature of 680 °C and an Argon pressure in the plasma of 1.7 μbar.

Fig. 4 shows the variation of the discharge parameters with the filament heating current. As expected, the extracted current increases proportional to the arc current. However, if the filament current exceeds a certain value, the discharge becomes unstable. Only approximately every second pulse of the applied arc voltage ignites a plasma. Indicative for this mixture operation mode are a still high arc voltage of 40 to 60 V and an extracted beam current of only 55 to 80 mA.

2.2.3 Pure Lithium Operation

When the temperature of the furnace exceeds $\sim$ 680 °C, the 100 kHz oscillations of the arc voltage suddenly disappear. The pulse only shows a small 300 Hz ripple, which is due to the arc current supply unit. These discharge parameters are distinctly different from those of the preceding modes. The arc voltage drops to 30 V and the arc current increases to 30 A. The smaller arc voltage must be due to the lower ionization potential of Li. The Ar gas feed can be totally closed and the filament heating current sometimes turned off. We attribute this to the transition of the discharge to a self-sustained arc with cathode spots. Even if argon were not totally shut off, the fraction of Ar in the beam should be small, because the ionization cross-section of Ar is smaller than that of Li.

The extracted ion current is as high as 120 mA. This is in accordance with the Child-Langmuir relation which predicts an increase with the inverse of the square-root of the atomic mass. However, the current does not exactly follow the $U^{3/2}$ law predicted by the same relation, but falls off faster with decreasing extraction voltage. This is because the lithium vapour pressure was kept constant, instead of being decreased by lowering the Li-oven temperature to get a perfect matching of the space charge limited flow [9].

The pulse-shape and the current density of the beam are sensitively controlled by the arc voltage, though the range allowing for stable operation of the arc is much smaller than for the other operation modes. Since the filament heating current as well as the arc power were dimi-

nished in this mode, the discharge chamber cools down. The temperature of the front reflector e.g. goes down to 410 °C. In order to prevent lithium from condensing on the walls and eventually forming a conducting bridge between cathode and anode, the heat input should be enhanced by increasing the duty-cycle of the arc. This is the only free parameter.

In the following, we estimate the vapour pressure of Li in the discharge chamber. During a normal run of 6 to 8 hours a layer of solid lithium is formed on the intermediate grid having a thickness of 1 to 2 mm. This originates from neutral lithium vapour escaping through the extraction holes with a flux 1/4 nv. We compare this flux with the area density of the Li layer devided by the operation time of the source, assume the ideal gas equation and a temperature of about 500 °C and calculate a pressure of 2.3 μbar. As expected, this is quite close to the argon pressure (see sec. 2.1).

Based on this number we deduce the temperature of the furnace necessary for supplying a sufficient inflow of lithium. In steady-state, the rate of lithium flowing into the discharge chamber must be equal to the loss rate of lithium. The latter is proportional to the area of the extraction holes and the area of the gap between the anode cylinder and the reflectors. With a gap of 2.5 mm the total area was calculated to 1500 mm^2. Equating the Li-flux through this area to the flux out of the tube connecting the furnace and the discharge chamber the vapour pressure in the furnace is determined to exceed 0.18 mbar, i.e. a temperature of 620 °C. The temperatures measured by a thermocouple ranged from 680 to 740 °C which implies a factor of 10 higher pressure. However, this is explained by the small conductance of the connecting tube [11] not considered in this estimate.

2.3 Limits of Working Time

2.3.1 Furnace Filling

The working time in the pure Li operation mode is given by several technical and physical limitations, one of which is the maximum filling

of the furnace. For a horizontal mounting of the source, it may only be filled by 2.7 g, since otherwise molten lithium flows through the connection tube and causes a short-circuit between anode and cathode. This filling should last for 5 to 6 hours estimated from the loss rate of lithium as explained in the preceding section.

This limitation implies that the furnace has to be opened and refilled after each run. This turned out to be rather difficult. The screw-cap of the furnace which is made out of molybdenum could not be removed because of freezing. In order to open the furnace, the whole ion source had to be dismounted. So we replaced the screw-cap by a flat cap of stainless steel with a thickness of 5 mm hold by four screws. Sealing was accomplished by a knife edge in the cap pressing a thin (0.1 mm) ring of tantalum. The screws of stainless steel may only be used once, since they reach their endurance limit at 700°C. This cap could be removed after a run without problems. However, there was another problem: Due to thermal stress the cap warped so that lithium leaked out of the furnace. The leakage was so high that sometimes no lithium was detected in the discharge chamber. This problem can hopefully be solved by reconstruction of the sealing with a cap made of molybdenum which has a better thermal stability.

2.3.2 Extraction System

After several hours of operation the intermediate grid is covered by a layer of solid lithium. Unfortunately, the diameter of the holes decreases, too, from 5 mm to about 3 or 4 mm. This diminishes the beam current and more significantly alters the extraction geometry, which causes the beam to defocus (see section 5). We observed a 50 % decrease of the current density within 3.5 hours. This time scale could only be improved by returning temporarily to the pure argon operation mode in order to clean the holes by sputtering. Naturally, the grids have to be cleaned e.g. by water after each run.

2.3.3 High Voltage Breakdown

For clean extraction grids of molybdenum or elkonite with well polished surfaces a gap of 3.5 mm is able to hold a voltage of 35 kV [8,12]. By operation with Li, however, it was not possible to obtain stable conditions above 20 kV. This is thought to be due to adsorption of Li, which has a very low electron affinity, on the grid surfaces. Therefore the extraction gap was increased to 7.5 mm, although this causes a drop in the extracted beam current.

Still, sometimes numerous voltage breakdowns occur during Li-operation. These events seem to happen mainly at the curved edge of the intermediate grid, which is evident from small circular footpoints at the circumference of the adjacent flange. As Li has a low electron affinity it is obvious that lithium must be prevented from diffusing to the edge of the intermediate grid, where the electric field strength is enhanced. This is achieved by keeping this grid so cool that lithium already condenses in the centre of it. We also found that breakdowns are more seldom when the argon pressure is low.

2.3.4 Anode-Cathode Short-Circuits

There is only a gap of 2.5 mm between anode and reflector which is on cathode potential (Fig. 1). Sometimes it may happen that the discharge voltage suddenly breaks down to a value of less than 5 V. This is partially caused by loose flakes of oxidized Li short-circuiting anode and cathode. At other times, protruding edges of the anode cylinder cause metal arcing. Arc tracks are readily observed on the front reflector. If this happens, the lithium or argon plasma extinguishes and the current is either conducted by the short-circuit or the metal arc. Usually, after the voltage has been switched off and the walls have been allowed to cool down slightly, the short-circuit is removed by itself. These events can be minimized, if the discharge chamber is carefully cleaned after each run. The anode cylinder has to be polished with fine emery and flakes have to be removed.

The filaments do hardly limit the working time of the source. The tantal filaments of the cathode have to be replaced after 2 to 3 runs, whereas the tungsten filaments of the furnace can be used much longer.

3. Charge Exchange Cell

The charge exchange cell used in the experiment is a rebuilt of that constructed by McCormick [5]. It looks like a double T, the upper bar of which is the active charge exchange cell with a diameter of 25 mm and a length of 120 mm. The charge exchange cell and the other beam line components for the beam diagnostics are shown in Fig. 6. The tube is heated by several windings of a coaxial heater wire. Contrary to the

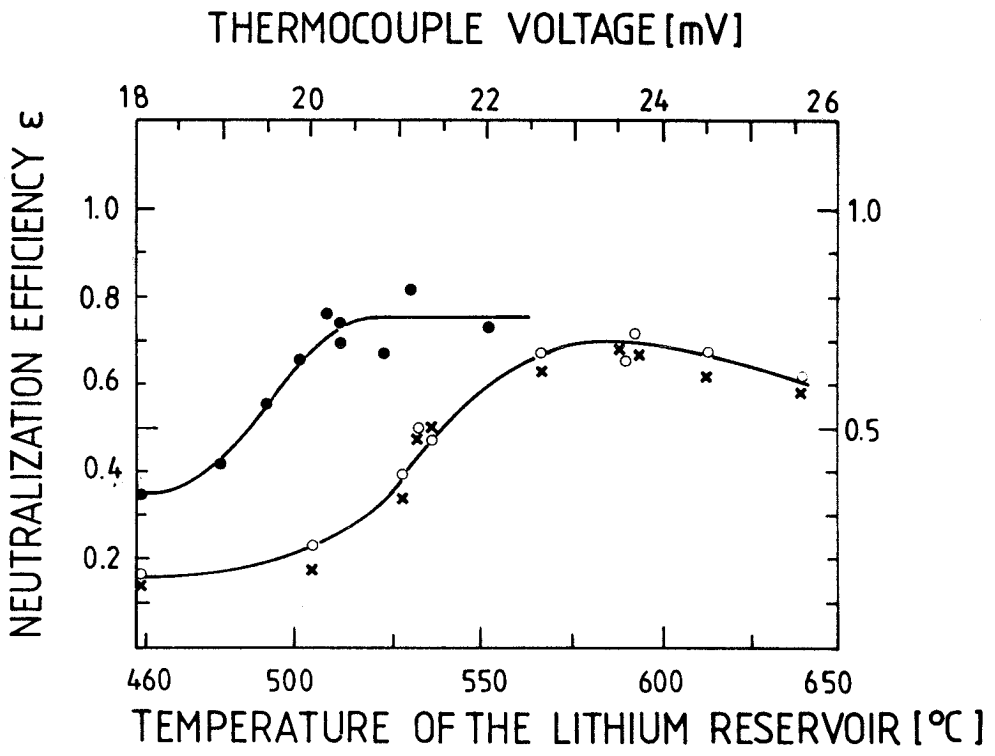

Fig. 5: Charge exchange efficiency as function of the temperature of the Li-reservoir from Faraday cup (x) and calorimetric measurements. The filled circles are determined with an extended neutralization cell.

original version, the length of the cell has been extended from 120 to 180 mm by stainless steel tubes pushed over the ends. This lowers the loss rate of the filling substance and increases the charge exchange efficiency (Fig. 5). The lower bar of the T is the reservoir with an independent heating circuit. This reservoir is filled with lithium.

The fraction of beam ions suffering a charge exchange collision in the cell is:

$$\varepsilon = I^{\circ}/I_{tot} = 1 - \exp(-L\,\sigma_{cx}\,n) \qquad (2)$$

L is the geometric length of the cell, σ_{ex} the charge exchange cross section and n the mean vapour density of lithium. For a mean pressure of 1 μbar or a density of 10^{13} cm^{-3} (see the appendix) and a charge exchange cross-section of 8×10^{-15} cm^2 [4], a neutral beam fraction of 0.76 is calculated, if reionization effects can be neglected. This fraction has actually nearly been achieved in the experiment (Fig. 5). For this pressure, the mean free path between two charge exchange collisions is about 13 cm compared to a tube length of 18 cm, so that reionization effects cannot totally be neglected.

From rough estimates of the pumping speed of the tube connecting the reservoir and the cell, McCormick calculated that the pressure in the reservoir must be a factor of 2.6 higher than that in the cell. We imply another factor of 2 in order to allow for a non-uniform distribution of the lithium density in the cell. Consequently, the lithium vapour pressure in the reservoir should exceed 5 μbar. Typically, we have heated the reservoir up to 530 °C and the cell slightly more, which corresponds to a pressure of 20 μbar. The difference is reasonable in view of the uncertainties of the estimate. The electric power for the cell and the reservoir is 200 W AC in either case. The cell is additionally heated by the ion beam itself.

The loss rate of lithium is given by the vapour pressure of Li and the pumping speed of the tubes [5]. Here we calculate a loss rate of about 30 μg/s. A filling of 2 g of lithium should last for 15 hours of continuous operation. Practically, we have refilled the cell for each run with

1 to 2 g. Therefore a considerable amount of lithium accumulated in the reservoir and had to be removed sometimes by water or even concentrated hydrochloric acid. The refills are necessary, because when opening the vacuum chamber lithium is covered by a nitride or oxide layer, which perhaps cannot be melted in a subsequent run.

Behind the cell there is an electro-magnet producing a magnetic field of maximum 0.06 T. This is sufficient to deflect the non-neutralized part of the beam onto a water cooled beam dump (Fig. 6).

4. Determination of the Neutral Beam Density

4.1 Methods

4.1.1 Faraday Cup

Usually, Faraday cups are used for the measurement of ion beam currents. However, for high beam current special care must be taken due to the screening of external potentials by the ion space charge [12,13]. This space charge is compensated by electrons produced at apertures or by ion impact ionization of the residual gas molecules [14]. Therefore the ion beam must be treated as a plasma with a flux of monoenergetic positive ions and an electron cloud of low energy electrons [15]. In order to measure the ion beam current correctly, these electrons must be prevented from entering the Faraday cup and the secondary electrons produced in the Faraday cup from leaving it. This is normally done by a negative external potential at the entrance of the Faraday cup. Due to the infavourable geometry and the high space-charge screening effect [12] this could not be fully guaranteed in the present case and some of the secondary electrons might have left the cup pretending a higher ion current. The effect was minimized by increasing the negative potential to -400 V, but may still be present. Fortunately, for the determination of the neutral beam flux, the ion current is of minor importance.

The neutral beam flux was measured in the following way. The bottom of the Faraday cup (in the following called the target) is disconnected from the surrounding Cu cylinder and biased by a potential of -30 V

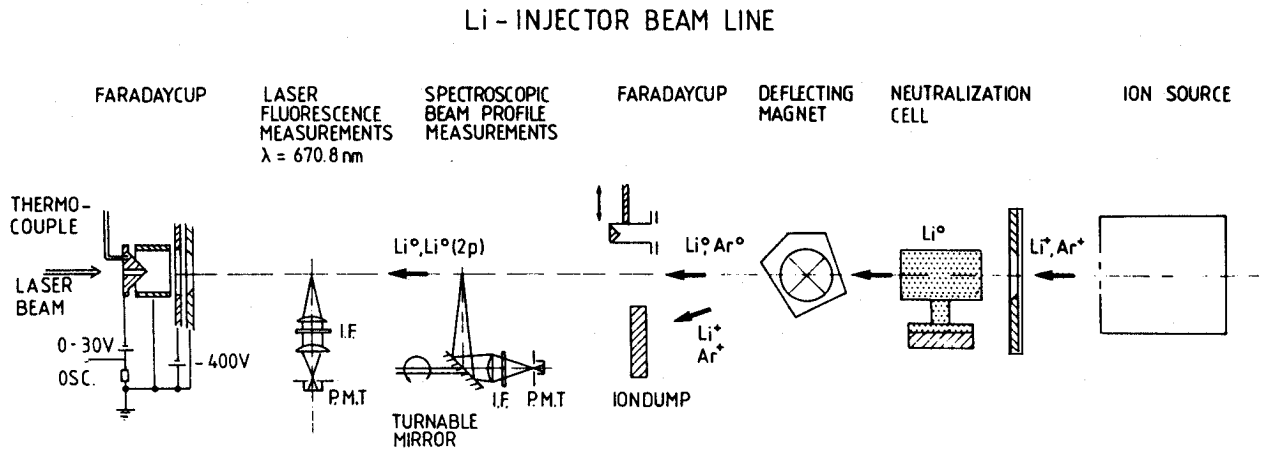

Fig. 6: Li-injector beam line components (not in scale). The distance from the ion source to the Faraday cups are 1.2 m and 1.9 m, respectively.

(Fig. 6). Because of this negative potential the electrons carried by the beam are repelled by the target. On the other side, the secondary electrons produced by ion bombardment all leave the target. Assuming the same electron emission coefficient γ for ions as well as for neutrals the current measured at the target consists of the secondary electron current plus the incident ion current:

$$I = \gamma (I^+ + I^0) + I^+ \qquad (3)$$

If one switches on the magnet behind the cell, the ions are deflected so that only the neutral particles come through. The current at the target then is:

$$I_B = \gamma I^0 \qquad (4)$$

I_B is indeed proportional to the neutral beam current, as is evident from Fig. 7. It is proportional to the energy deposited by the neutrals as measured by the thermocouple as well as to the collision induced Li I fluorescence light. From the ratio of the two currents I and I_B the degree of neutralization of the beam is obtained:

$$\varepsilon = I_B/(I - I^+) = I^\circ/(I^\circ + I^+) \qquad (5)$$

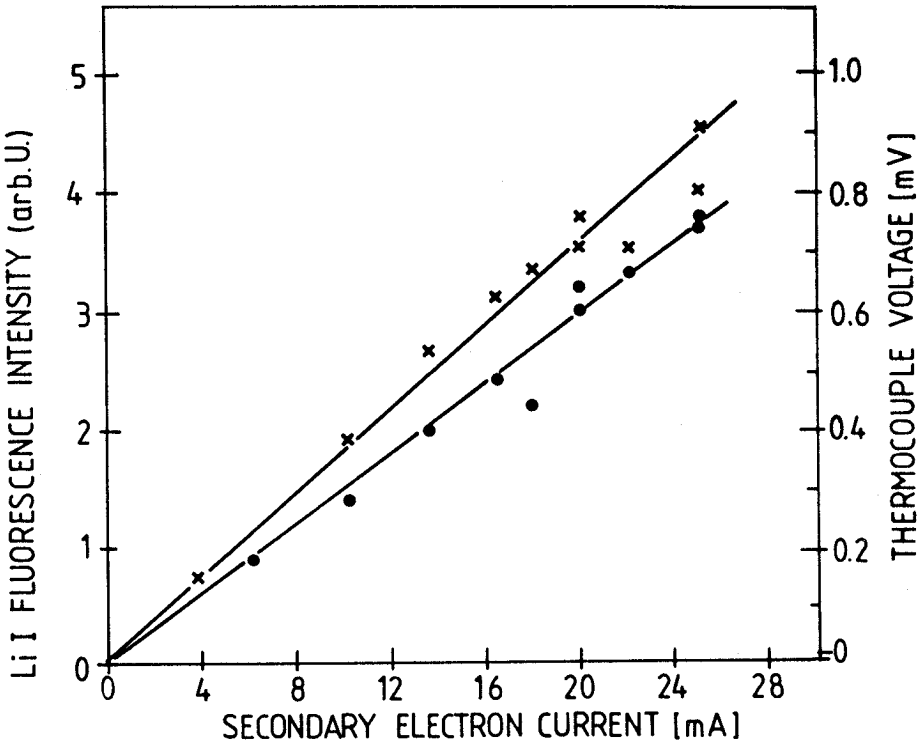

Fig. 7: Li I fluorescence intensity at 670.8 nm (o) and temperature rise measured by the thermocouple (x) (see Fig. 6) for different secondary electron currents I_B at the Faraday cup (neutrals only).

If some neutral atoms are reionized on their way to the Faraday cup, this ion current has to be subtracted from I_B. Inserting the measured value of I^+, which may be an overestimation, a lower limit of the neutralization efficiency is obtained. Fig. 5 shows the conformity of the efficiencies determined from the Faraday cup currents and those measured by the calorimeter.

The neutral beam current can be obtained from the neutralization efficiency ε and the ion current I^+:

$$I^\circ = I^+ \cdot \varepsilon/(1 - \varepsilon) \qquad (6)$$

However, this equation sensitively relies on a proper determination of I^+. This is circumvented, if the neutral current is directly deduced from the target current I_B of the Faraday cup provided γ is exactly

known. Therefore we would like to determine the secondary emission coefficient γ independently. In the simplest case, when no neutrals are reionized, γ is given by:

$$\gamma = (I - I^+ - I_B)/I^+ \qquad (7)$$

If reionization occurs, this ion current has to be subtracted from I_B allowing for an upper limit of γ. The preceding equation again suffers from the uncertainty in I^+. However, for the determination of γ, the beam current can be made arbitrary small. In this case, space charges are small and the ion current measured at the Faraday cup should be more reliable. Therefore the measurement was repeated with an ion beam reduced to a diameter of 5 mm by an aperture in front of the cup. The secondary emission coefficient was determined to 4 to 5 for Ar, which is consistent with ref. 16. For Li, we obtained a value of 1.6 to 2.5, which is also used in ref. 6. In the following, we will use the latter value.

4.1.2 Calorimeter

A calorimeter [17] measures the deposited energy or power by measuring the temperature rise. The measurement is independent of whether ions or neutrals are detected and introduces only a small error due to reflected atoms. We used a crude version of a calorimeter consisting of the target of the Faraday cup (Fig. 6) with a Chromel-Alumel thermocouple inserted into it. Electrons do not influence the energy balance, since they have much smaller energies. For currents of 10 mA and duty-cycles of 50 %, a temperature rise of 20 °C was observed. The thermal time constant is determined by the effectiveness of the water cooling of the target and turned out to be 30 to 60 s. The temperature linearly increased with the beam current. In principle, it is possible to calibrate this calorimeter by a well-known heat source, as e.g. a resistive heater built into the target, but here only its proportional characteristic was used. The neutralization efficiency of the charge exchange cell was determined from the ratio of the target temperature obtained with the total beam and the neutrals only (Fig. 5). For this, the deflecting magnet behind the cell has to be switched off and on, respectively.

4.1.3 Fluorescence Light

The Faraday cup as well as the calorimeter do not distinguish between Li and Ar, which may be present in operation mode B. An analysing magnet was not available for us. Instead, we used the collision induced fluorescence light of Li I at 670.8 nm, which is directly proportional to the neutral current density j of lithium alone.

$$F_{coll} \sim A_{21} \cdot (j/e) \cdot n_{gas} \cdot \sigma_{exc} \cdot V \cdot d\Omega \qquad (8)$$

A_{21} is the transition probability, n_{gas} the density of the background gas, σ_{exc} the proper excitation cross-section, V the observation volume and $d\Omega$ the solid angle of the detection system. This consists of two imaging lenses, an interference filter for selecting the Li I line or a monochromator, a slit of 2 mm x 4 mm defining V and a standard photomultiplier (RCA 1P28A) (Fig. 6). We also measured the spatial profile of the fluorescence light. For this, the slit-width was reduced to 0.1 mm, and a motor-driven mirror was inserted into the detection optics so that the slit could be scanned over a definite portion of the beam. In order to obtain absolute values of the beam density, the excitation cross-section of the Li I line, the pressure of the background gas and the overall sensitivity of the optical system have to be known.

Another possibility is provided by laser induced fluorescence spectroscopy [18,19]. The intense light of a dye-laser is used for the excitation of the Li I line with the laser frequency on resonance. For the short pulses of flashlamp-pumped dye-lasers, the fluorescence light is proportional to the neutral density n of Li I:

$$F_{laser} \sim (g_2/(g_1+g_2))(S/(1+S))\ n\ A_{21}\ V\ d\Omega \qquad (9)$$

g_i are the statistical weights of the pumped levels and S is the saturation parameter. The product of the lithium neutral density n, the velocity v, and the charge e gives the neutral current density j:

$$j = e\ n\ v \qquad (10)$$

For absolute numbers, the fluorescence intensity has to be calibrated e.g. by Rayleigh scattering which only requires the knowledge of the laser power density and the gas pressure. The Li I transition 2 S - 2 P at 670.8 nm facilitates the calibration procedure, since it involves only two levels, i.e. the excited state and the groundstate.

Some comments have to be made on the saturation parameter S [18,19]. Taking the lowering of the pumping efficiency due to the comparatively short time the fast particles are illuminated into account a value of 10 was calculated. The atoms cross the laser beam, which is aligned perpendicular to the ion beam, in a time x/v, where x is the diameter of the laser beam. Also, the fluorescence light is transported into the direction of the neutral beam due to the high velocity of the Li atoms and the 27 ns lifetime of the excited Li I level. For the calibration only that part of the scattering volume must be imaged, which is illuminated by the laser beam. The Rayleigh light originates from almost resting thermal nitrogen molecules, which do not radiate outside the laser beam. The mode structure of the laser frequency spectrum introduces a correction giving up to 40% higher neutral densities[18,19].

Last not least, a fraction of 9 % has to be added to the calculated density due to the isotope ^{6}Li. This is not excited by the laser light, but detected in the Faraday cup. In view of the discussion above the uncertainty of the laser fluorescence measurement was estimated to $\sim$ 50 %.

4.2 Results

The neutral beam current is computed from I_B/γ for $\gamma = 2.5$. The mean beam current density is the ratio of the neutral current and the area of the opening of the cup. The density in the centre of the beam should even exceed this number. Current densities obtained this way are compared to those measured by laser induced fluorescence 1.6 m from the ion source (Table 2) for three different runs. Obviously, the latter method gives the lower current densities ranging from 0.4 to 2.2 mA/cm^2. Referring to the classification of the ion source operation modes this

Table 2

Neutral current densities for three different runs obtained from Faraday cup (A) and laser fluorescence (B) measurements

	RUN: 1	2	3	unit
extr. ion current	79	89	106	mA
Li neutr. density (B)	2.8	3.9	15.0	$10^7/cm^3$
Li current density (B)	0.4	0.56	2.2	mA/cm^2
current density (A)	1.1	1.3	3.1	mA/cm^2
Li fraction	36	44	71	%

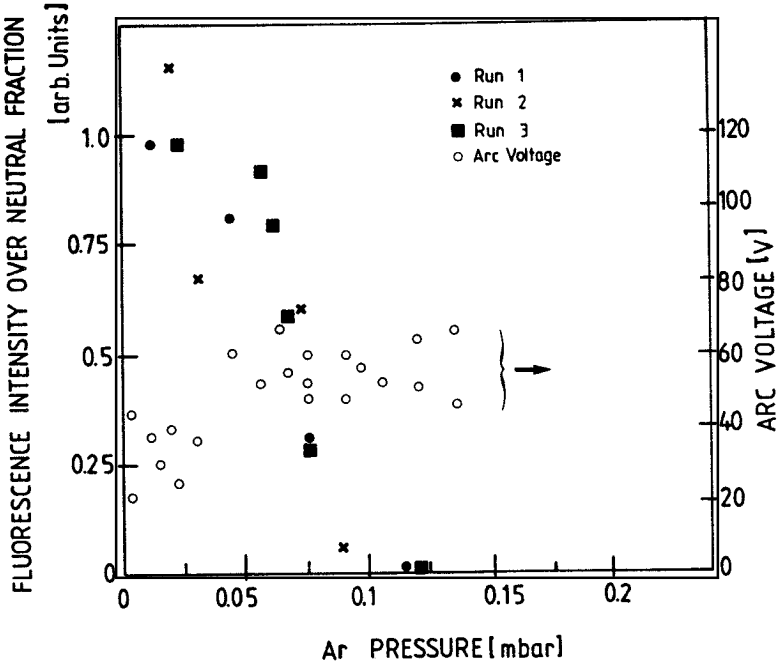

Fig. 8: Ratio of the Li I fluorescence intensity to the neutral fraction of the extracted currents versus the Ar pressure as measured at the gas feed. The points belong to three different runs. The shift in the arc voltage (o) indicates the transition from mode B to mode C at pressures below 0.05 mbar.

confirms that Li is only a fraction of the total extracted beam. This fraction increases with increasing total current, i.e. when going from mode B to mode C.

Fig. 8 shows the ratio of the Li I fluorescence light to the total neutral beam (calculated from the extracted beam current and the neutralization efficiency ε) for different argon pressures in the source. From the right to the left side of the figure the furnace temperature increases implying a reduction in the argon pressure. The computed ratio, which is proportional to the fraction of Li in the beam increases with decreasing Ar pressure and saturates for pressures smaller than 0.045 mbar at the gas feed. In this case, the Li fraction should be close to 100 %. On the other hand, for the operation of the source with Ar pressures of more than 0.09 mbar, the fraction of Li is smaller than 10 %. The pure Ar operation mode is achieved for 0.12 mbar.

5. Determination of the Li-Beam Divergence

The collision induced fluorescence light of Li I allows for the determination of the current density profile of the neutral beam and its divergence angle.

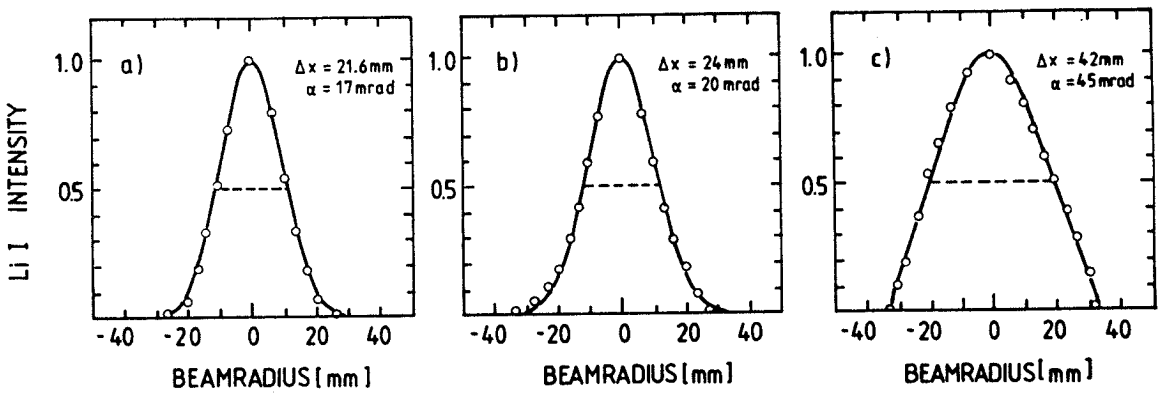

Fig. 9: Spatial profiles of the Li I intensity at a distance of 0.85 m from the source. The full lines are calculations using the indicated value of the beam divergence α. The operation time increases from Figure a) to c).

Knowing the divergence and the total extracted current one has the possibility to calculate the beam current density at any given distance to the source. Thus, we can easily check the ion current measured with the Faraday cup.

The spatial profiles of the Li I fluorescence intensity at 670.8 nm obtained by means of the scanning mirror are plotted in Fig. 9. The Gaussian half-width range from 21.6 to 42 mm. The increased half-width indicates the defocussing of the beam, when the extraction holes of the intermediate grid are filled with condensed lithium. Fig. 10 shows how the half-width of the beam increases during the operation of the source.

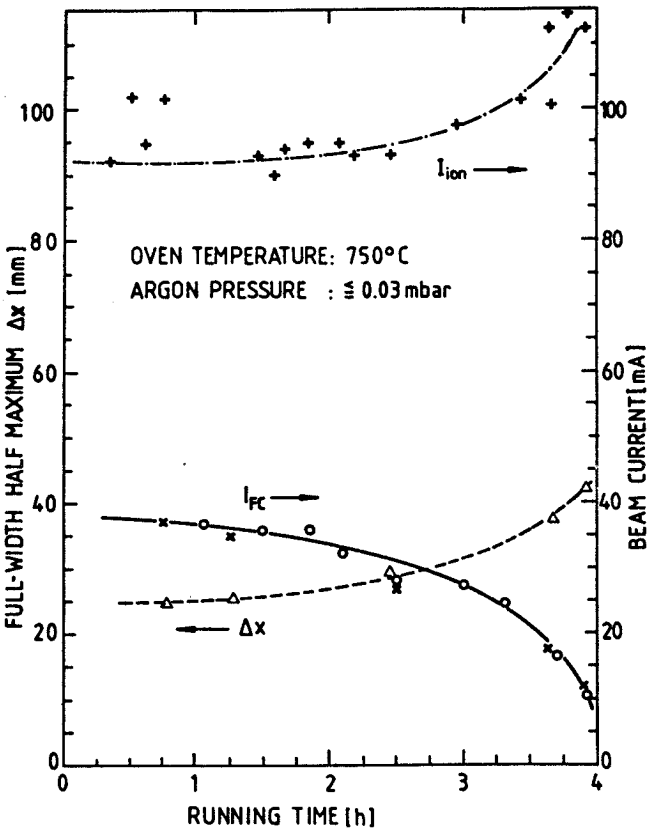

Fig. 10: Extracted beam current I_{ion}, local current measured at the Faraday cup I_{FC}, and full-width half-maximum of the spatial beam profile during a run of the ion source.

At the same time, the current measured within the 25 mm opening of the Faraday cup decreases. However, this run was an extreme case. In other runs, the drop of the current density was delayed by a factor of 2.

The measured beam profiles are compared with a numerical superposition of seven Gaussian beam profiles emerging paraxially from the holes of

the extraction system. The half-width of these beamlets is assumed to vary like:

$$\Delta x = d + \alpha z \qquad (11)$$

z is the distance to the source, d the diameter of the holes and α the full divergence angle of a single beamlet. Fig. 11 shows the calculated full half-width of the complete beam as function of z and α. The Li I profiles are consistent with a full divergence angle of 17.5 to 20 mrad. We have also calculated the relative decrease of the current passing through a circular aperture of 25 mm diameter as function of the distance z. This dependence can be directly compared with the current measured at various distances by the Faraday cup, which has an opening of the same size. From the data taken at three different distances (0.85, 1.2 and 1.9 m) marked as points in Fig. 11 a divergence angle of 20 to 30 mrad is deduced. This is larger than that determined from the spatial profile of the beam. However, the smaller currents at z = 1.9 m provoking a higher divergence could be assigned to alignment errors or to a considerable fraction of Ar in this particular run. Ar has a slightly higher divergence than Li. From measurements of the spatial distribution of an Ar I line, we deduced a divergence angle of 27 to 30 mrad for Ar.

The half-widths of the profiles increase strongly, if e.g. the negative potential on the intermediate extraction grid is lowered so far that the current reading of the HV power supply shows a dramatic increase. In this case, a significant electron current is drawn into the source distorting the space charge compensation of the beam and causing its defocussing.

The beam width hardly changed when the beam energy was decreased from 30 to 15 keV. Similarly for high neutralization efficiencies, when the vapour pressure in the charge exchange cell was high, the half-width decreased by at most 8 %. It is concluded that the beam broadening by multiple scattering was negligible. The observed reduction of the half-width may be due to a better compensation of the space charge of the incoming ion beam.

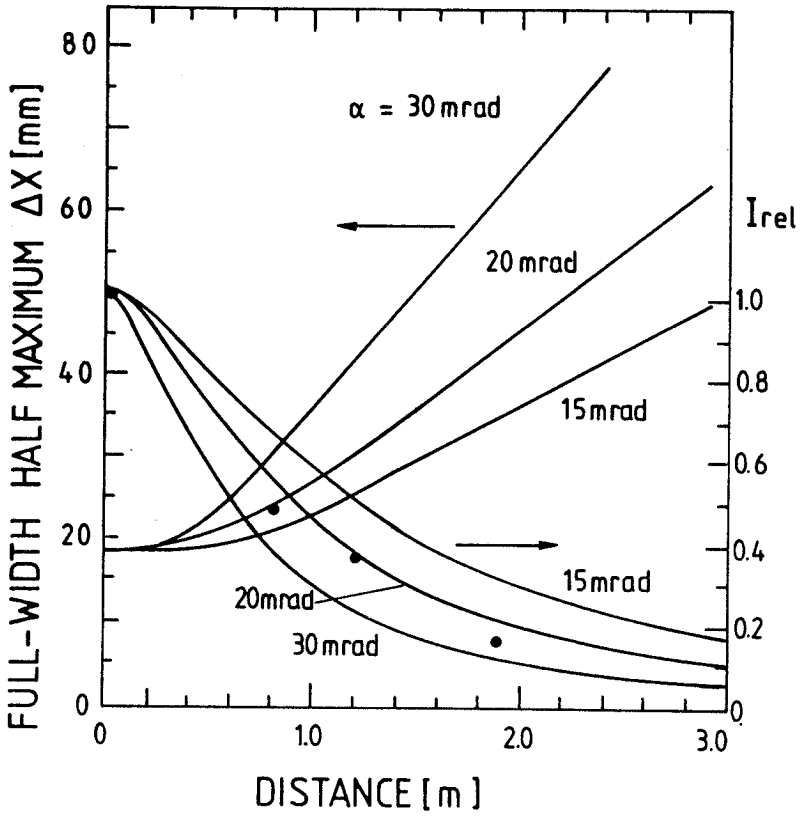

Fig. 11: Calculated full-width half-maximum Δx of the beam profile and the beam current I_{rel} within a diameter of 25 mm relative to the total extracted current I_{ion} as a function of the distance from the source for three different beam divergence angles. The filled points show measured currents I_{rel} at different positions of the Faraday cup.

6. Summary

We have optimized the parameters of a low-pressure arc ion source operated with lithium in order to get the highest current densities. We have found three modes of operation distinguished by the fraction of lithium in the beam. The mode achieving a fraction of up to 100 % of Li naturally is the most desirable of the three. However, in this mode the working time of the source is determined by several technical and physical limitations, as e.g. the limited filling of the lithium furnace, the condensation of lithium on the extraction grids, the increasing

probability of short-circuits between anode and cathode and high voltage breakdowns.

In the following Table 3 the optimum values of the current density, the beam divergence and neutralization efficiency achieved here are quoted. The data have been taken from calorimetric, Li I line intensity, laser fluorescence and Faraday cup measurements as described and discussed in the text.

Table 3

Achieved optimum neutral beam parameters at 30 keV

Extracted total current:	90 - 120 mA
Neutralization efficiency:	70 %
Half-width at a distance of 0.9 m:	24 mm
Full beam divergence:	20 - 25 mrad
Li current density	
at a distance of 1.9 m:	2.1 mA/cm^2
at a distance of 1.2 m:	4.5 mA/cm^2

Acknowledgements

The present work was done under the auspices of the Sonderforschungsbereich Nr. 162 Bochum - Jülich. One of the authors (H.L. Bay) is very grateful to R. Keller and to the GSI, Darmstadt, for the very intensive and helpful cooperation during the first tests of the ion source in Darmstadt.

Appendix

In the following, we list some useful formulas. The temperature T must be inserted in K, the pressure p in mbar, throughout. M designates the atomic mass number.

The current escaping from the boundary of a plasma of density n is:

$$j = (1/4)\, n\, \bar{v}\, e$$

$\bar{v}$ is the thermal velocity of the particles given in m/s:

$$\bar{v} = (8\ kT/\pi m)^{1/2} = 146\ (T/M)^{1/2}$$

The Child-Langmuir law in practical units reads (U is the extraction voltage inserted in kV and l the extraction gap width in cm):

$$j = 1.7\ (1/M^{1/2})\ U^{3/2}/l^2 \quad [mA/cm^2]$$

The vapour pressure of lithium corresponding to the temperature T is [5]:

$$\log P = 7.62 - 7480/T$$

The density of particles given in cm^{-3} corresponding to a pressure P and temperature T is:

$$n = 7.25 \times 10^{18}\ P/T$$

The number of particles contained in a piece of metal of mass m measured in g is:

$$N = 6.02\ .\ 10^{23}\ m/M$$

The Chromel-Alumel thermocouple voltage U given in mV is converted into the temperature T measured in °C by (it has to be corrected eventually for the room temperature):

$$T = 23.7\ U$$

The melting and boiling temperatures of lithium are:

$$T = 180.6\ °C \qquad \text{and} \qquad T = 1347\ °C$$

References

/1/ K. Kadota, K. Tsuchida, Y. Kawasumi, J. Fujita: Plasma Physics 20, 1011 (1978)

/2/ H. Winter: Comments on Modern Physics D 12, 165 (1982)

/3/ F. Aumayr, M. Fehringer, H. Winter: J. Phys. B 17, 4185 (1984)

/4/ H. Tawara, T. Kato, G. Nakai: Report IPPJ-AM-30, Inst. of Plasma Phys. Nagoya, Japan

/5/ K. McCormick: Report IPP III/82 (1983), Max-Planck-Institut für Plasmaphysik, Garching

/6/ K. McCormick, M. Kick: Report IPP III/85 (1983), Max-Planck-Institut für Plasmaphysik, Garching

/7/ P.G. Weber: Rev. Sci. Instr. 54, 1506 (1983)

/8/ R. Keller, P. Spädtke, F. Nöhmayer in: Proc. Int. Ion Engineering Congress, Kyoto (1983), p. 25

/9/ I. Langmuir, K.T. Compton: Rev. Mod. Phys. 3, 191 (1931)

/10/ H.R. Kaufmann, I.M.E. Harper, I.I. Cuomo: J. Vac. Sci. Technol. 16, 899 (1979)

/11/ M. Wutz, H. Adam, W. Walcher: "Theorie und Praxis der Vakuumtechnik", Friedr. Vieweg Verlag, Braunschweig (1982)

/12/ C.M. McKenna: Radiat. Eff. 44, 93 (1979) and C.M. McKenna: in H. Ryssel, H. Glawischnig (eds.) "Ion Implantation: Equipment and Techniques" Springer Series in Electrophysics Vol. II, Springer Verlag, Berlin, Heidelberg, New York (1983), p. 73

/13/ J.E. Osher: Inst. Phys. Conf. Ser. No 38, 201 (1978)

/14/ A.J.T. Holmes: Inst. Phys. Conf. Ser. No 38, 222 (1978)

/15/ F.F. Chen: "Introduction to Plasma Physics and Controlled Fusion, Vol. 1, Plasma Physics", Plenum Press, New York (1984)

/16/ A. von Engel, M. Steenbeck: "Elektrische Gasentladungen", Vol. I & II, Springer Verlag (1932-34)

/17/ J.O. Olsen, N. Andersen, T. Andersen: J. Phys. B 10, 1723 (1977)

/18/ E. Dullni, Report Jül-1936 (1984), KFA Jülich

/19/ W. Berres, D. Rusbüldt, E. Hintz, H.L. Bay, Appl. Phys. B35, 83 (1984)